

CENTRAL ASIAN JOURNAL OF MEDICAL AND NATURAL SCIENCES

https://cajmns.centralasianstudies.org/index.php/CAJMNS

Volume: 06 Issue: 04 | October 2025 ISSN: 2660-4159



Article

Temperature Dependence of Photoluminescence and Calculation of Activation Energy for Thermal Quenching in Cspbbr₃ Perovskite

M. O. Rahmonova*1, N. Q. Mukhamadiev1, Yu. G. Galyametdinov2

- 1. Samarkand State University named after Sharof Rashidov, Uzbekistan
- 2. Kazan National Research Technological University, Kazan, Russia
- * Correspondence: rakhmanovashirin@gmail.com

Abstract: This paper investigates the temperature dependence of the photoluminescence properties of inorganic perovskite CsPbBr₃. Nanoparticles were synthesized by a ligand-assisted method using CsBr and PbBr₂ as precursors, dimethyl sulfoxide as a solvent, and oleylamine and oleic acid as stabilizers. After purification by centrifugation with acetone, the samples were analyzed using a Shimadzu RF-6000 spectrofluorometer in the temperature range of 45–95 °C. With increasing temperature, the photoluminescence peak shifts from 448 nm (2.77 eV) at 45 °C to 567 nm (2.19 eV) at 95 °C. Simultaneously, the spectral line broadens from ~30 to ~40 nm (FWHM), and the emission intensity decreases by more than half. These changes result from band gap narrowing, enhanced electron–phonon coupling, and activation of defect states. The activation energy of non-radiative processes was calculated as Ea≈0.374 eV, consistent with literature data. The results clarify the mechanisms of thermal quenching in CsPbBr₃ and are relevant for perovskite-based optoelectronic devices.

Keywords: CsPbBr₃, Photoluminescence, Temperature, Red Shift, FWHM, Activation Energy, Temperature Decay

Galyametdinov, Y. G. Temperature dependence of photoluminescence and calculation of activation energy for thermal quenching in

CsPbBr3 perovskite. Central Asian

Journal of Medical and Natural Science 2025, 6(4), 2379-2385.

Citation: Rahmonova, M. O., Mukhamadieva, N. Q., &

Received: 13th Sept 2025 Revised: 20th Sept 2025 Accepted: 04th Oct 2025

Published: 13th Oct 2025



Copyright: © 2025 by the authors. Submitted for open access publication under the terms and conditions of the Creative Commons Attribution (CC BY) license

(https://creativecommons.org/licenses/by/4.0/)

1. Introduction

In recent years, inorganic halide perovskites, especially CsPbBr₃, have attracted increased attention from researchers due to their unique optical and electrochemical properties. These materials are characterized by high photoluminescent quantum efficiency, narrow spectral line width, and the ability to change the bandgap width by altering the composition or size of nanoparticles [1], [2], [3], [4]. Because of these features, CsPbBr₃ is considered a promising material for use in light-emitting diodes, solar cells, lasers, photodetectors, and sensor devices [5], [6], [7], [8], [9]. However, despite its impressive characteristics, one of the main problems remains the instability of perovskites when exposed to external factors such as temperature, moisture, and oxygen. When heated, a decrease in the intensity of photoluminescence (PL) is observed, a shift of its maximum emission towards longer wavelengths, and a broadening of spectral lines. These effects are associated with the activation of non-radiative recombination channels, the enhancement of electron-phonon interactions, and the involvement of defect states [10], [11], [12], [13], [14], [15]. It is known that temperature effects in perovskites are effectively described by the Varshen equation, which relates the band gap width to temperature [16],

[17], [18], [19], [20]. As the temperature increases, the width of the forbidden zone decreases, causing a red shift in the photoluminescence maxima. Moreover, the contribution of phonon processes increases, causing line broadening and enhanced quenching. To quantitatively estimate thermal quenching, the activation energy (Ea) is calculated, which reflects the depth of defect levels and thermally activated traps. For CsPbBr₃, values in the range of 0.2–0.4 eV are given in the literature, which confirms the model of activation of non-radiative recombination pathways [21], [22], [23], [24]. Determining the activation energy has both fundamental and applied significance. From a fundamental point of view, it helps to understand the mechanisms of degradation of perovskite compounds. From a practical point of view, it makes it possible to predict the stability and efficiency of perovskite light-emitting diodes and other optoelectronic devices under various operating conditions. Accordingly, the current task is to study the temperature dependence of CsPbBr₃ photoluminescence in the range of 45–95 °C and to determine the activation energy of thermal quenching.

This work is aimed at analyzing PL spectra at three temperature states, identifying patterns of λ max maximum shift and line broadening, and calculating the activation energy of non-radiative processes.

2. Materials and Methods

Cesium bromide (CsBr, 99.9%, Sigma-Aldrich), lead bromide (PbBr₂, 99.9%, Alfa Aesar), dimethyl sulfoxide (DMSO, analytical grade), oleylamine (OAm, 70%), oleic acid (OA, 90%), and acetone (as a precipitant, pure for analysis). All reagents were used without additional purification. Preparation of the precursor solution. A stoichiometric amount of CsBr and PbBr₂ in a molar ratio of 1:1 was dissolved in 10 ml of DMSO at a temperature of 85 °C. To stabilize the colloidal particles, oleylamine and oleic acid were added to the mixture in equal volumes (0.3 ml each). The mixture was stirred with a magnetic stirrer at a constant speed until the components were completely dissolved.

To isolate the nanoparticles, acetone was added to the reaction mixture in a volume exceeding the initial solution by 3–4 times. Precipitation occurred as a result of a decrease in the solubility of perovskite compounds. The resulting suspension was then centrifuged at 6000 rpm for 10 minutes. The separated precipitate was redispersed in toluene until a transparent colloidal solution was obtained. Photoluminescence measurement. Photoluminescence spectra were recorded on a Shimadzu RF-6000 spectrofluorometer. The sample temperature was controlled with an accuracy of ± 0.5 °C. Measurements were performed at three temperatures: 45, 65, and 95 °C. The spectra were recorded in the range of 400–800 nm. The maximum emission values (λ max), full width at half maximum (FWHM), and relative integral intensity were taken for analysis.

To calculate the activation energy of thermal quenching, the following model was used:

$$I(T) = \frac{I_0}{1 + A_{exp}(-E_a/k_BT)}$$

Where I0 is the limiting intensity at low temperature, A is an empirical constant, kB is Boltzmann's constant, and Ea is the activation energy. Linearization of the equation allowed us to plot the dependence of ln(I0/I-1) on 1/T and determine the value of the activation energy from the slope of the line.

3. Results and Discussion

The photoluminescent properties of CsPbBr₃ were studied in the temperature range of 45–95 °C. The obtained spectra showed regular changes in the position of the emission maximum, the width of the spectral lines, and the intensity.

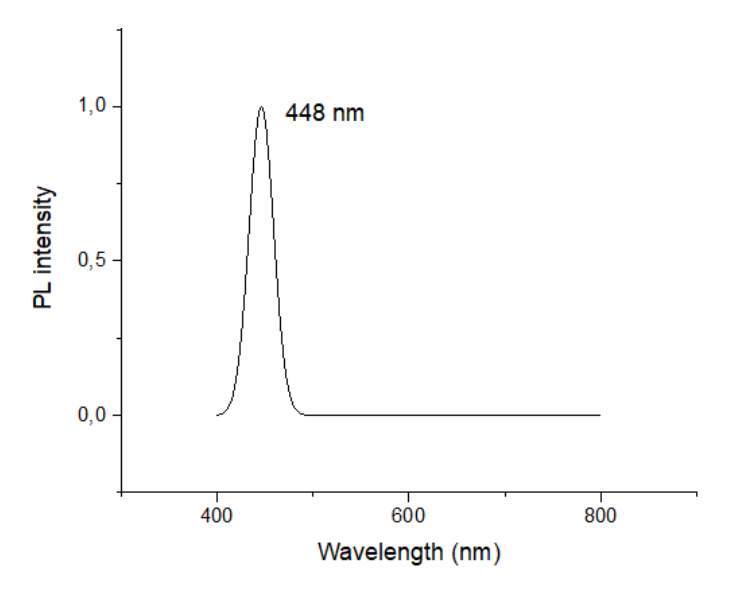


Figure 1. Photoluminescence spectrum of CsPbBr₃ at 45 °C.

At 45 °C (Figure 1), the maximum photoluminescence was recorded at 448 nm (2.77 eV). The spectrum was narrow (FWHM \approx 30 nm) and the intensity was high, indicating the predominance of radiative recombination.

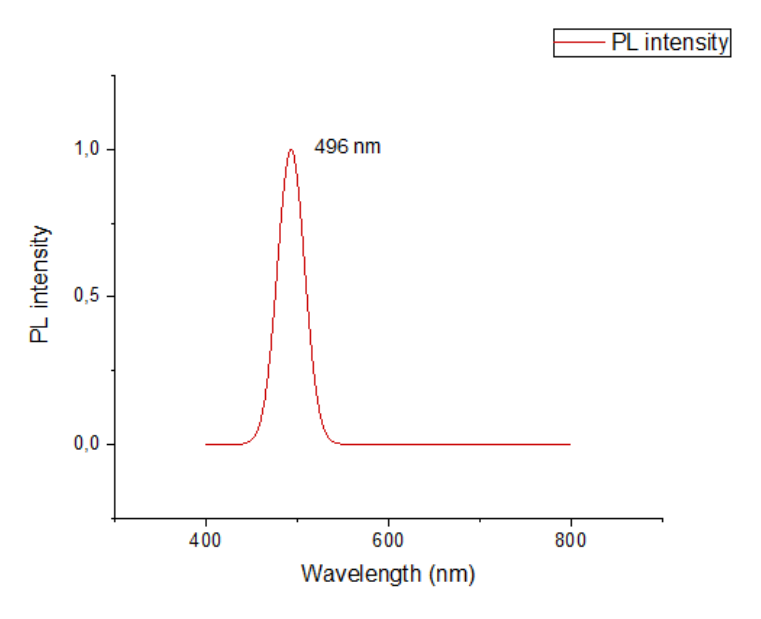


Figure 2. Photoluminescence spectrum of CsPbBr₃ at 65 °C.

At 65 °C (Figure 2), the maximum shifted to the long-wave region (496 nm, 2.50 eV), and the line width increased to \sim 35 nm. At the same time, a decrease in intensity of approximately 30% was observed. These changes indicate the onset of thermal quenching caused by electron-phonon interaction and activation of trap levels.

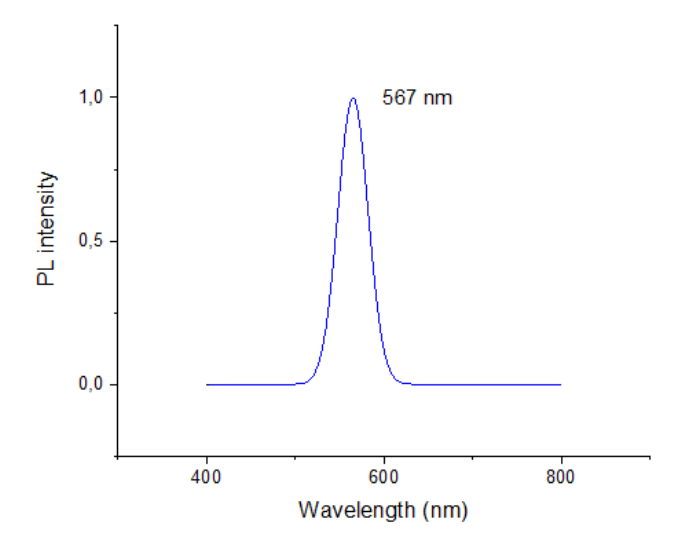


Figure 3. Photoluminescence spectrum of CsPbBr₃ at 95 °C.

Further heating to 95 $^{\circ}$ C (Figure 3) resulted in a red shift of the maximum to 567 nm (2.19 eV). The line width increased to \sim 40 nm, and the intensity fell by more than half relative to the initial value. This reflects the increase in the contribution of non-radiative processes and the high sensitivity of the material to heating.

Table 1. Photoluminescence parameters of CsPbBr₃ under various temperatures.

Temperature, °C	λmax, nm	Photon energy, eV	FWHM, nm	Relative intensity	Spectrum characteristics
45	448	2.77	~30	1.00	Narrow peak in the blue region; high intensity, minimal extinction
65	496	2.50	~35	0.70	Red shift into the blue- green region; onset of thermal quenching, increase in phonon contribution
95	567	2.19	~40	0.45	Strong red shift into the yellow-green region; pronounced quenching, activation of defective states

Comparative data are presented in Table 1. It can be seen that λ max systematically shifts to the long-wave region, FWHM increases, and intensity decreases. Figure 4 shows these dependencies in graphical form: as the temperature increases, the radiation maximum shifts by approximately 120 nm, and the line width increases by ~30%.

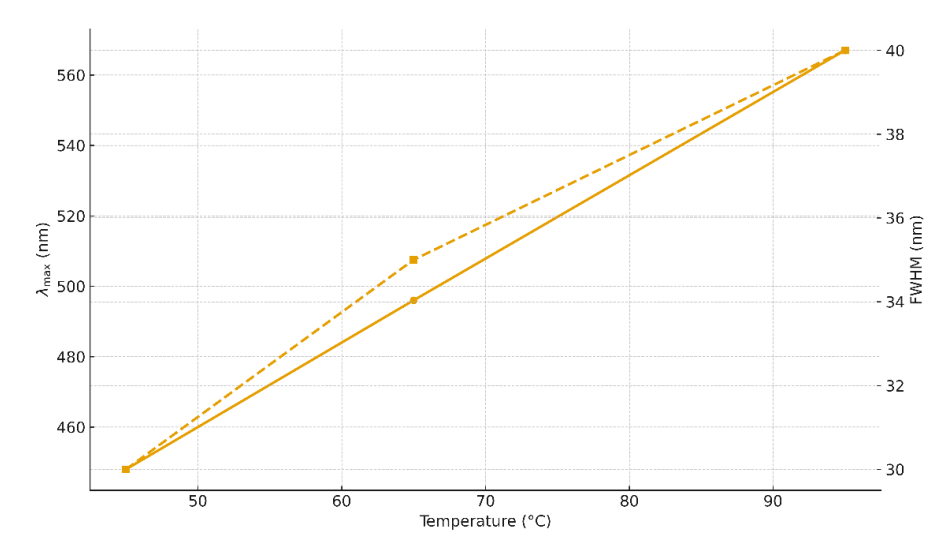


Figure 4. Temperature dependence of the position of the photoluminescence maximum (λ max) and spectral line width (FWHM) in CsPbBr₃.

For quantitative analysis, the activation energy was calculated using the photoluminescence thermal quenching model. Linearization of the dependence of $\ln(I0/I-1)$ on 1/T (Figure 5) allowed us to determine the activation energy $Ea\approx0.374~eV~(\approx374~meV)$. This value is consistent with the literature data (0.2–0.4 eV), which confirms the activation of defect states as the main mechanism for reducing intensity during heating.

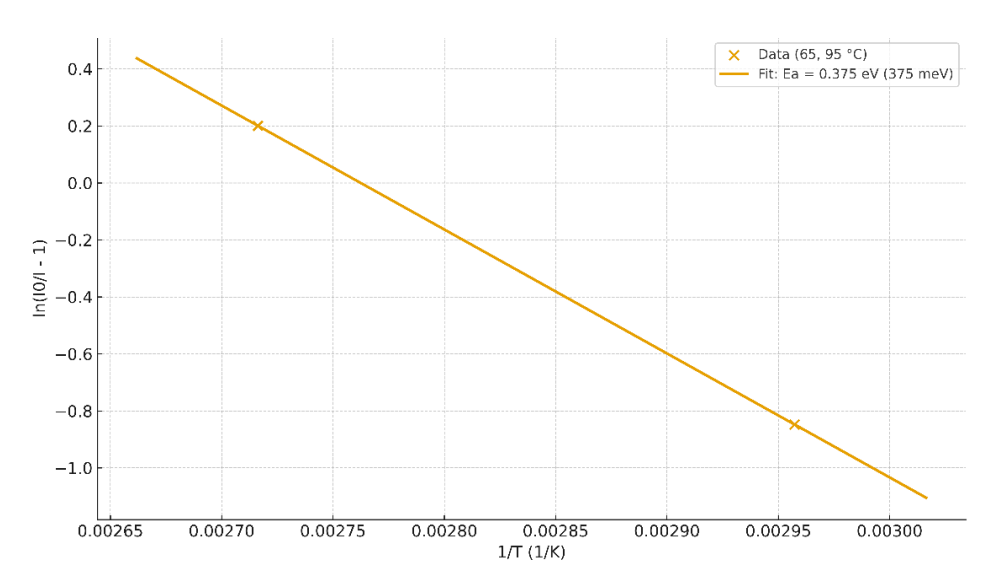


Figure 5. Linearization of CsPbBr₃ photoluminescence thermal quenching.

Thus, the results obtained show that the key factors in the degradation of photoluminescence in CsPbBr₃ are a decrease in the bandgap width, an increase in electron-phonon interaction, and an increase in the contribution of defect levels with rising temperature. This limits the effectiveness of the material in light-emitting devices and highlights the need to develop methods for stabilizing the structure.

4. Conclusion

It has been established that when the temperature rises from 45 to 95 $^{\circ}$ C, the photoluminescence of CsPbBr₃ shifts from 448 to 567 nm, which corresponds to a decrease in photon energy from 2.77 to 2.19 eV.

The temperature increase is accompanied by a broadening of the spectral lines (FWHM increases from ~30 to ~40 nm) and a significant decrease in radiation intensity.

Based on the results of linearization of thermally quenched photoluminescence, the activation energy of non-radiative processes was calculated to be ~0.374 eV.

The data obtained confirm that the key reasons for the degradation of photoluminescence in CsPbBr₃ are a decrease in the bandgap width, electron-phonon broadening, and activation of defect levels.

REFERENCES

- [1] L. Protesescu, S. Yakunin, M. I. Bodnarchuk, and M. V. Kovalenko, "Nanocrystals of cesium lead halide perovskites (CsPbX₃, X = Cl, Br, I): Novel optoelectronic materials showing bright emission with wide color gamut," *Nano Letters*, vol. 15, no. 6, pp. 3692–3696, 2015, doi: 10.1021/nl5048779.
- [2] M. V. Kovalenko, L. Protesescu, and M. I. Bodnarchuk, "Properties and potential optoelectronic applications of perovskite nanocrystals," *Science*, vol. 358, no. 6364, pp. 745–750, 2017, doi: 10.1126/science.aam7093.
- [3] Q. A. Akkerman, G. Rainò, M. V. Kovalenko, and L. Manna, "Genesis, challenges and opportunities for colloidal lead halide perovskite nanocrystals," *Nature Materials*, vol. 17, no. 5, pp. 394–405, 2018, doi: 10.1038/s41563-018-0018-4.
- [4] S. Yakunin, L. Protesescu, F. Krieg, *et al.*, "Low-threshold amplified spontaneous emission and lasing from colloidal nanocrystals of caesium lead halide perovskites," *Nature Communications*, vol. 6, article 8056, 2015, doi: 10.1038/ncomms9056.
- [5] M. O. Rakhmonova, *et al.*, "Poluchenie i svoystva pektina iz otkhodov pishchevoy promyshlennosti," *Universum: Khimiya i Biologiya*, no. 3-2(105), pp. 13–19, 2023, doi: 10.32743/UniChem.2023.105.3.14990.
- [6] M. O. Rahmonova, A. M. Zufarov, and N. K. Muxamadiev, "Synthesis and analysis of the optical properties of the perovskite material KPbBr₃: Studying the characteristics and potential for application," *American Journal of Biodiversity*, vol. 1, no. 6, pp. 6–10, 2024.
- [7] H. Zhu, B. Shao, Z. Shen, S. You, J. Yin, N. Wehbe, *et al.*, "In situ energetics modulation enables high-efficiency and stable inverted perovskite solar cells," *Nature Photonics*, vol. 19, no. 1, pp. 28–35, 2024, doi: 10.1038/s41566-024-01542-8.
- [8] M. Shin, J. Kim, Y. K. Jung, T.-P. Ruoko, A. Priimägi, A. Walsh, *et al.*, "Low-dimensional formamidinium lead perovskite architectures via controllable solvent intercalation," *Journal of Materials Chemistry C*, vol. 7, no. 13, pp. 3945–3951, 2019, doi: 10.1039/c9tc00379g.
- [9] A. A. Petrov, A. A. Ordinartsev, S. A. Fateev, E. A. Goodilin, and A. B. Tarasov, "Solubility of hybrid halide perovskites in DMF and DMSO," *Molecules*, vol. 26, no. 24, article 7541, 2021, doi: 10.3390/molecules26247541.
- [10] C. C. Stoumpos, D. H. Cao, D. J. Clark, J. Young, J. M. Rondinelli, J. I. Jang, et al., "Ruddlesden–Popper hybrid lead iodide perovskite 2D homologous semiconductors," *Chemistry of Materials*, vol. 28, no. 8, pp. 2852–2867, 2016, doi: 10.1021/acs.chemmater.6b00847.
- [11] N. Ashurov, B. L. Oksengendler, S. E. Maksimov, S. Rashiodva, A. R. Ishteev, D. S. Saranin, *et al.*, "Current state and perspectives for organo-halide perovskite solar cells: Crystal structures and thin film formation, morphology, processing, degradation, stability improvement by carbon nanotube," *Materials of Electronics Engineering*, vol. 20, no. 3, pp. 153–193, 2017, doi: 10.17073/1609-3577-2017-3-153-193.
- [12] L. Budzhemila, A. N. Aleshin, V. G. Malyshkin, P. A. Aleshin, I. P. Shcherbakov, V. N. Petrov, and E. I. Terukov, "Electrical and optical characteristics of lead halide perovskite nanocrystal films CsPbI₃ and CsPbBr₃ deposited on c-Si solar cells for photovoltaic applications," *Physics of the Solid State*, vol. 64, no. 11, pp. 1695–1700, 2022, doi: 10.21883/ftt.2022.11.53322.418.
- [13] A. N. Aleshin, I. P. Shcherbakov, D. A. Kirilenko, L. B. Matyushkin, and V. A. Moshnikov, "Light-emitting field-effect transistors based on composite films of polyfluorene and CsPbBr₃ nanocrystals," *Physics of the Solid State*, vol. 61, no. 2, pp. 388–392, 2019, doi: 10.21883/ftt.2019.02.47142.244.

- [14] A. V. Ivanchikhina and K. S. Pundikov, "Comparative analysis of synthesis methods for CsPbBr₃ perovskite nanoparticles at room temperature," *High Energy Chemistry*, vol. 54, no. 5, pp. 361–369, 2020, doi: 10.31857/s0023119320050071.
- [15] S. M. H. Qaid, H. Murtaza, Q. Ain, M. U. Din, H. M. Ghaithan, A. Ali, et al., "The physical attributes of rubidium-based Rb₂TlRhF₆ double perovskite halide: A first-principles investigation," *Physica B: Condensed Matter*, vol. 685, article 416000, 2024, doi: 10/j.physb.2024.416000.
- [16] T. He, Y. Jiang, X. Xing, and M. Yuan, "Structured perovskite light absorbers for efficient and stable photovoltaics," *Advanced Materials*, vol. 32, no. 26, article 1903937, 2020, doi: 10.1002/adma.201903937.
- [17] G. Li, F. Wisnivesky, S. Bai, T. C. Jellicoe, F. Ayala, *et al.*, "Highly efficient perovskite nanocrystal light-emitting diodes enabled by a universal crosslinking method," *Advanced Materials*, vol. 28, no. 18, pp. 3528–3534, 2016, doi: 10.1002/adma.201600064.
- [18] N. J. Jeon, J. H. Noh, W. S. Yang, Y. C. Kim, S. Ryu, J. Seo, et al., "Compositional engineering of perovskite materials for high-performance solar cells," *Nature*, vol. 517, no. 7535, pp. 476–480, 2015, doi: 10.1038/nature14133.
- [19] X. Li, Y. Wu, S. Zhang, B. Cai, Y. Gu, J. Song, *et al.*, "CsPbX₃ quantum dots for lighting and displays: Room-temperature synthesis, photoluminescence superiorities, underlying origins and white light-emitting diodes," *Advanced Functional Materials*, vol. 26, no. 15, pp. 2435–2445, 2016, doi: 10.1002/adfm.201600109.
- [20] G. Niu, X. Guo, and L. Wang, "Review of recent progress in chemical stability of perovskite solar cells," *Journal of Materials Chemistry A*, vol. 3, no. 17, pp. 8970–8980, 2015, doi: 10.1039/C4TA04994B.
- [21] L. Dou, A. B. Wong, Y. Yu, M. Lai, N. Kornienko, S. W. Eaton, et al., "Atomically thin two-dimensional organic-inorganic hybrid perovskites," *Science*, vol. 349, no. 6255, pp. 1518–1521, 2015, doi: 10.1126/science.aac7660.
- [22] G. E. Eperon, G. M. Paternò, R. J. Sutton, A. Zampetti, A. A. Haghighirad, F. Cacialli, et al., "Inorganic caesium lead iodide perovskite solar cells," *Journal of Materials Chemistry A*, vol. 3, no. 39, pp. 19688–19695, 2015, doi: 10.1039/c5ta06398a.
- [23] J. H. Heo, H. J. Han, D. Kim, T. K. Ahn, and S. H. Im, "Hysteresis-less inverted CH₃NH₃PbI₃ planar perovskite hybrid solar cells with 18.1% power conversion efficiency," *Energy & Environmental Science*, vol. 8, no. 5, pp. 1602–1608, 2015, doi: 10.1039/c5ee00120j.
- [24] S. Sun, D. Yuan, Y. Xu, A. Wang, and Z. Deng, "Ligand-mediated synthesis of shape-controlled cesium lead halide perovskite nanocrystals via reprecipitation process at room temperature," *ACS Nano*, vol. 10, no. 3, pp. 3648–3655, 2016, doi: 10.1021/acsnano.5b08193.